Korean J. of Chem. Eng., **5**(2) (1988) *154-163*

ON THE HEAT TRANSFER MECHANISM IN THREE PHASE FLUIDIZED BEDS

Yong KANG and Sang Done KIM*

Department of Chemical Engineering, Chungnam National University, Taejon 302-764, Korea
*Department of Chemical Engineering, Korea Advanced Institute of Science and Technology, Seoul 137-791, Korea

(Received 26 September 1987 • accepted 6 November 1987)

Abstract—A two resistance model is proposed for the heat transfer between a coaxially mounted heater and a three phase fluidized bed.

Effects of gas and liquid velocity and particle size on individual heat transfer resistances in the heater and in the fluidized bulk zones have been determined.

The optimum bed porosity at which the maximum heat transfer coefficient occurred coincided with the bed porosity at which the boundary layer thickness around the heater attained a minimum value. The fluidized bed resistance attained its minimum value when the maximum heat transfer coefficient is achieved in two and three phase fluidized beds.

The heat transfer in the zone adjacent to the heater is found to be the rate controlling step since the contribution of fluidized bed resistance was found to be less than 10% of the heater zone resistance in two and three phase fluidized beds.

The heat transfer resistances in liquid and three-phase fluidized beds have been represented by a modified Stanton and Peclet numbers based on the heat transfer resistances in the heater zone and in the fluidized bulk zone in series.

INTRODUCTION

In tubular reactors such as a fluidized bed reactor, the reaction temperature has been efficiently controlled by cooling or heating the wall of the column. In either a continuous or batch reactor, it is possible to install a heating or cooling element in the bed to maintain the desired bed temperature.

Dockwer[1] examined the heat transfer mechanism in bubble column reactor using the surface renewal model and the isotropic turbulence theory.

Lewis et al.[2] have proposed a simple mathematical model for heat transfer in a bubble column using the concept of unsteady state heat diffusion.

Chen and McMillan[3] suggested the analogy between the axial heat transfer and the axial dispersion of liquid phase in a batch bubble column. In gas-liquid system, it has been generally known that the unsteady state heat diffusion takes place from the fluid elements adjacent to the heater wall.

In a liquid fluidized bed, a series model for wall-to-bed heat transfer was proposed by Wasmund and Smith[4]. These authors found that the wall thermal resistance increased with the increase in bed porosity. Richardson et al.[5] have correlated the j-factor in terms of a modified Reynolds number and reported that the presence of particles might improve the heat transfer in liquid fluidized beds since the particles tend to disturb the boundary layer at the heat transfer surface.

From wall-to-bed heat transfer data, Patel and Simpson[6] suggested that the principal mechanism of heat transfer in liquid fluidized beds is the fluid eddy convection, in contrast to the particle carrier mechanism for gas fluidized beds. The heat transfer coefficient was found to be independent of the height above the distributor. In three phase fluidized beds, heat transfer characteristics have been studied on wall-to-bed[7-11] and on heater-to-bed[12-14] systems. Muroyama et al.[11] have determined the wall-to-bed heat transfer coefficient based on an axial dispersion model. The unsteady state heat diffusion model[14, 15] was used to analyze the heat transfer between the immersed heater and the three phase fluidized beds.

In the present study, a two-resistance model based on the radial dispersion of a continuous liquid phase is presented to describe the heat transfer mechanism in

three phase fluidized beds.

HEAT TRANSFER MODEL

The radial temperature profile in the zone adjacent to the heater is much steeper than in the fluidized bulk zone[10].

This may imply that there are two resistances for heat transfer in three phase fluidized beds, namely heater surface resistance and the fluidized bed resistance in a manner similar to the heat transfer mechanism in liquid fluidized beds[4,6,16].

The similar trend in the radial temperature profile between liquid and gas-liquid fluidized beds may suggest that a gas injection into the liquid fluidized bed may reduce the resistances.

A two resistance model is proposed for the analysis of heat transfer between an immersed heater and three phase fluidized beds with the following assumptions;

1) The thermo-physical properties of fluid and solid are constant. 2) The heat transfer operation is in a steady state. 3) The heater surface temperature is uniform. 4) the coaxial thermal boundary layer thickness around the heater has an average value in a fully developed steady state condition. 5) The temperature gradient at the wall of the bed is negligible. 6) The overall resistances of heat transfer consists of a resistance of heater surface and a resistance of the bulk fluidized bed in series. 7) The heat conduction is occurs in the thermal boundary layer around the heater[17]. 8) The velocity profile in the bed is flat in a steady state condition [10,18]. The two resistance model can be described as

$$\frac{1}{h} = \frac{1}{h_h} + R_b \tag{1}$$

where h, h_h and R_b are the overall heat transfer coefficient, heat transfer coefficient in the heater zone and heat transfer resistance in the fluidized bulk zone, respectively. A schematical representation of the present model can be seen in Fig. 1.

The heat balance of the continuous liquid phase in the infinitesimal annulus of the bed leads to

$$U_l \rho_l C_{pl} \frac{\partial T}{\partial z} = D_z \rho_l C_{pl} \frac{\partial^2 T}{\partial z^2} + \frac{1}{r} \frac{\partial}{\partial r} \left(D_r C_{pl} r \cdot \frac{\partial T}{\partial r} \right) \tag{2}$$

where U_l, ρ_l, C_{pl}, D_r and D_z are the liquid velocity, liquid density, heat capacity of liquid, radial and axial dispersion coefficients, respectively.

In Eq.(2), T is a function of both z and r directions. However, for a fully developed flow in the constant heat flux, the temperature profiles increase linearly in the z-direction and T can be split into the sum of a z-dependent term $T_z(z)$ and an r-dependent term $T_r(r)$ as

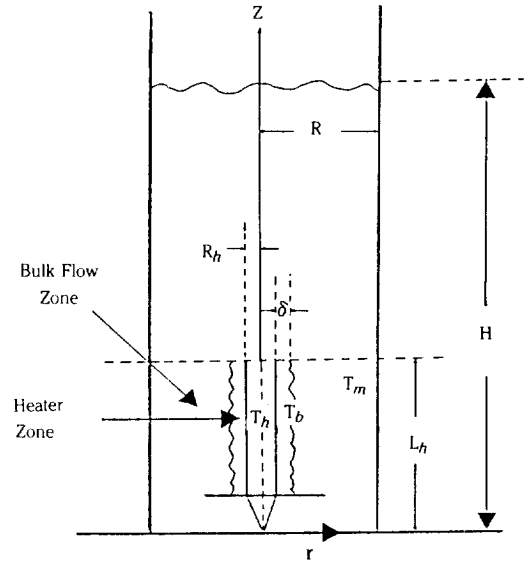

Fig. 1. Schematic diagram of heat transfer model.

$$T(r, z) = T_z(z) + T_r(r) \tag{3}$$

where $T_z(z)$ is the cross sectional averaged bulk temperature. Then, the left-hand side of Eq. (2) can be written as

$$U_l \rho_l C_{pl} \frac{\partial T}{\partial Z} - D_z \rho_l C_{pl} \frac{\partial^2 T}{\partial Z^2} = U_l \rho_l C_{pl} \frac{dT_z}{dZ} - D_z \rho_l C_{pl} \frac{d^2 T_z}{dZ} \tag{4}$$

From the steady-state heat balance on the incremental volume in the axial direction with the assumption of negligible heat loss through the bed wall, the following equation can be obtained[19]

$$(R^2 - R_h^2) \left(U_l \rho_l C_{pl} \frac{dT_z}{dZ} - D_z \rho_l C_{pl} \frac{d^2 T_z}{dZ^2} \right) = q/L_h = q_h \tag{5}$$

where R, R_h, L_h and q_h are the column diameter, heater diameter, heater length and the heat supply per unit time and unit length of the heater surface.

Since the present model is based on the constant heat flux, Eq. (5) represents the heat transferred from the heater surface to the bed in the axial direction due to the bulk flow of liquid and the thermal diffusion. The right hand side of Eq. (2) can be written as from Eq. (3),

$$\frac{1}{r} \frac{\partial}{\partial r} \left(D_r \rho_l C_{pl} r \frac{\partial T}{\partial r} \right) = \frac{1}{r} \frac{d}{dr} \left(D_r \rho_l C_{pl} r \frac{dT_r}{dr} \right) \tag{6}$$

Therefore, from Eqs. (4),(5), and (6), the following equation can be obtained with the following boundary conditions;

$$\frac{1}{r}\frac{d}{dr}\left(r\frac{dT_r}{dr}\right)=\frac{q_h}{\pi(R^2-R_h^2)D_r\rho_l C_{pl}} \tag{7}$$

$$\text{at } r=R_h+\delta \quad T(r,z)=T_b=T_h-\frac{q}{h_h A} \tag{8}$$

$$\text{at } r=R \quad \frac{dT_r}{dr}=0 \tag{9}$$

where δ is the average boundary layer thickness.

The first boundary condition can be obtained from the heat balance around the heater surface as

$$q=h_h(T_h-T_b)A \tag{10}$$

where A, T_b and q are the surface area of the heater, temperature at the thermal boundary layer around the heater and the heat flux from the heater to the bed.

From the solution of Eq. (7), the temperature profile in the bed and its mean value can be represented as in Eqs. (11) and (12), respectively.

$$\frac{T(r)-T_w}{T_h-T_w}=R_r\ln\frac{R}{r}-\frac{1}{2}(R^2-r^2)/\left\{\frac{(R_h+\delta)^2}{2}\left[1-\left(\frac{R}{R_h+\delta}\right)^2\right]+R^2\ln\left(\frac{R}{R_h+\delta}\right)\right\}+\frac{(R^2-R_h)^2 DrC_{pl}\rho_l}{R_h h_h} \tag{11}$$

$$T_h-T_m=\frac{q}{2\pi(R^2-R_h^2)D_r\rho_l C_{pl}L_h}\left\{\frac{R^2(R^2\ln R-R_h^2\ln R_h)}{R^2-R_h^2}-R^2\ln(R_h+\delta)+\frac{(R_h+\delta)^2}{2}-\frac{1}{4}(3R^2+R_h^2)\right\}+\frac{q}{Ah_h} \tag{12}$$

where the subscripts h, w, and m denote the heater surface, bed wall and the mean values, respectively. Therefore, the individual and the overall heat transfer resistances can be written as

$$\frac{1}{h}=\frac{A(T_h-T_m)}{q}=\frac{1}{h_h}+\frac{R_h}{(R^2-R_h^2)D_r\rho_l C_{pl}}\left\{\frac{R^2(R^2\ln R-R_h^2\ln R_h)}{R^2-R_h^2}-R^2\ln(R_h+\delta)+\frac{(R_h+\delta)^2}{2}-\frac{1}{4}(3R^2+R_h^2)\right\} \tag{13}$$

The resistance in the fluidized bulk zone can be determined as

$$R_b=\frac{R_h}{(R^2-R_h^2)D_r\rho_l C_{pl}}\left\{\frac{R^2(R^2\ln R-R_h^2\ln R_h)}{R^2-R_h^2}-R^2\ln(R_h+\delta)+\frac{(R_h+\delta)^2}{2}-\frac{1}{4}(3R^2+R_h^2)\right\} \tag{14}$$

Since the average boundary layer thickness around the heater is very thin relative to the bed radius, the steady state heat conduction takes place in the boundary layer as

$$h_h=k_l/\delta \tag{15}$$

where k_l is the thermal conductivity of the liquid phase. In three phase fluidized beds, Eq. (13) can be represented in terms of the dimensionless groups as

$$\frac{1}{St_M}=\frac{1}{St_{hM}}+KPe_{rM} \tag{16}$$

where St_M, St_{hM}, K and Pe_{rM} are the modified Stanton numbers in the fluidized zone and the heater zone, a constant and a modified Peclet number based on the radial dispersion coefficient of liquid phase, respectively.

EXPERIMENTAL

Experiments were carried out in a relatively large QVF glass column of 3 m high and 0.152 m in diameter as shown in the previous publication[13] A cone shape heater (3.0 cm-OD × 35.6 cm-long) as a heating source was placed vertically on the distributor plate at the center of the column.

In order to measure the radial temperature profile in the bed, five iron-constantan thermocouples were placed radially 20 cm above the distributor plate. The first thermocouples was located at 5 mm from the heater surface and the radial intervals were 5, 10, 20, and 21 mm. Each thermocouple was connected to a digital thermometer.

The used solids were either 1.7 or 4.0 mm glass beads with a density of 2500 kg/cm^3.

Air and water were introduced into the bed of solids with the desired superficial velocities and heat input. When a steady state was reached, the pressure profile up to the entire height of the column was measured using water manometers. The bed height was taken as the point at which a change in the slope of the plot was observed [13,20].

At the same time five bed temperatures and heater surface temperatures as well as the temperature in radial direction were continuously recorded(Molytek 1701). The heat transfer coefficient was calculated from the following equation:

$$h=\frac{q}{A(T_h-T_m)} \tag{17}$$

in which q is the heat flux from the heater to the bed and A is the effective surface area of the heater. T_h and T_m are the temperatures of heater surface and fluidized bed, respectively.

The temperature difference between the immersed heater and the bed has been determined by;

$$T_h-T_m=\frac{\int_o^R U(r)\,(T_h-T(r))\,rdr}{\int_o^R U(r)\,rdr} \tag{18}$$

Since the flat velocity profile can be assumed in multiphase fluidized beds[10,18], the values of heat flux, q, from the power supplier can be evaluated by the energy balance equation as

$$q = \dot{m} C_{pl} (T_{m,i} - T_{m,o}) \quad (19)$$

where $\dot{m}$ and C_{pl} are the mass flow rate of liquid phase and heat capacity, respectively. $T_{m,i}$ and $T_{m,o}$ are the temperatures of the inlet and the outlet positions, respectively.

RESULTS AND DISCUSSION

The radial temperature profile in Eq. (11) is a function of the average boundary layer thickness which can be obtained from the boundary layer temperature (Eqs. 10 and 15). The boundary layer temperature can be obtained from the intercept of the radial temperature profile extrapolated to the heater surface since the boundary layer is a very thin liquid film around the heater. Therefore, the average thickness and the temperature of the boundary layer were determined by a trial and error method in Eqs. (10),(11) and (15). The radial temperature profiles thus obtained are shown in Fig. 2 with the experimental data of the radial temperature profiles. For the sake of comparison, the data in liquid fluidized bed[6] and in three phase fluidized bed[10] were plotted in Fig. 2. As can be seen in the figure, the agreement between the values from Eq. (11) and the experimental values is excellent. This may indicate the temperature gradient at the wall of the bed is negligibly small.

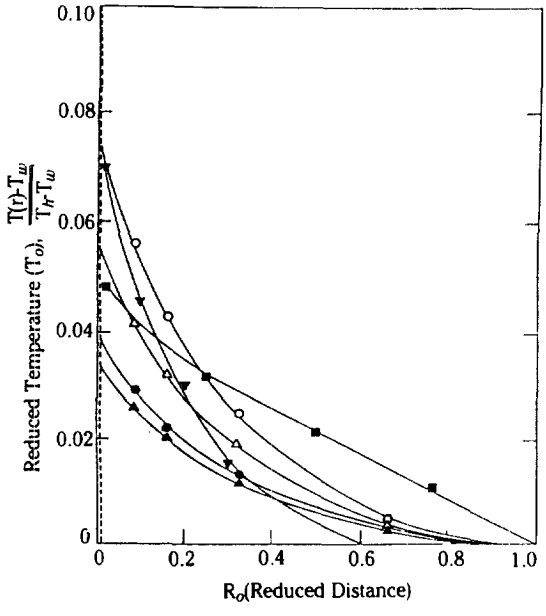

Fig. 2. Radial temperature profile in liquid and three-phase fluidized beds.

	○	●	△	▲	■	▼
d_p(mm):	1.7	1.7	4.0	4.0	3.2×3.2	0.579
	glass beads				r-alumina	lead sphere
U_g(cm/s):	4.0	6.0	8.0	10.0	7.6	ε_f 0.57-0.95
U_g(cm/s):	0.0	4.0	0.0	4.0	9.2	0.0
	present study				Chiu & Ziegler [10]	Patel & Simpson [6]

The heat transfer coefficients in the heater zone, h_h, were calculated from either Eq. (10) or (15) with the obtained values of the average boundary layer thickness and its temperature. The calculated heat transfer coefficients in the heater zone increased with an increase in gas velocity and in particle size. The average boundary layer thickness around the heater decreased with increasing gas velocity and particle size(Fig. 3A, 3B) since the heater zone heat transfer coefficient is inversely proportional to the average boundary layer thickness under the assumption that the heat conduction is the predominating heat transfer mechanism in the heater zone [17].

The average boundary layer thickness around the heater can also be determined experimentally from the measured boundary layer temperature, T_b, which was determined by extrapolating the radial temperature profile to the heater surface as the way done by Wasmund and Smith[4] and Patel and Simpson[6] in liquid fluidized beds using Eqs. (10) and (15). Thus, the obtained heat transfer coefficient in the heater zone and the average thermal boundary layer around the heater are shown in Fig. 3. As can be seen, the experimental values agree well with the theoretical values. It may suggest that the addition of gas into the liquid fluidized bed enhances the intensity of turbulence due to the vigorous bubbling motion in the bed which results in the decrease of average boundary layer thickness around the heater in a three phase fluidized bed. This may induce an increase of fluid element velocity which may provide the increased contacting frequency between the fluid element and the heater surface which in turn may results in a decrease in the average boundary layer thickness in the bed. The increase in heat transfer coefficient in the heater zone with particle size may be attributed to the reduction of boundary layer thickness around the heater[10,12,13].

The average boundary layer thickness around the heater exhibited a minimum value with liquid velocity in two and three phase fluidized beds as shown in Fig. 4B in which the solid line is the model line. In this figure, the minimum value of the thickness can be attained at liquid velocity of 8 cm/s for 1.7 mm particle whereas the minimum value of the thickness was attained at liquid velocity of 10 cm/s for 4 mm particle

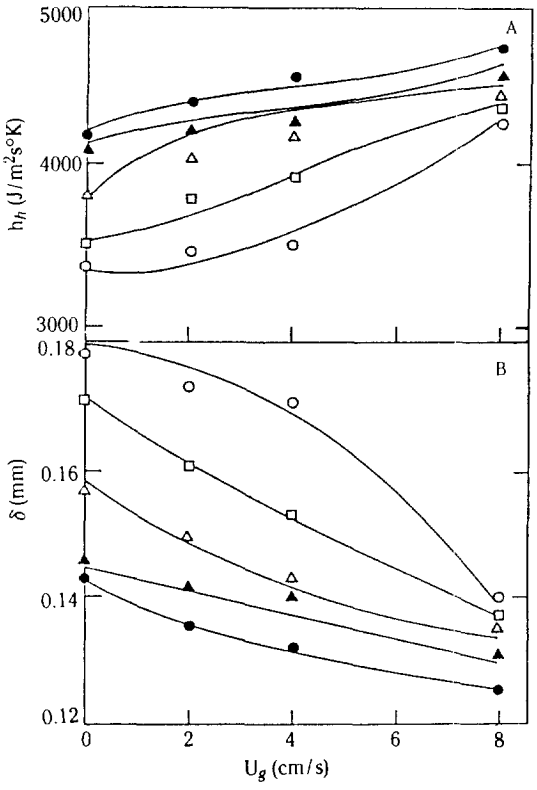

Fig. 3. Effect of gas velocity on the average thermal boundary layer thickness and the heat transfer coefficient in the heater zone.

	○	△	□	●	▲	——
d_p(mm):	1.7	1.7	1.7	4.0	4.0	model
U_l(cm/s):	4.0	8.0	10.0	10.0	12.0	

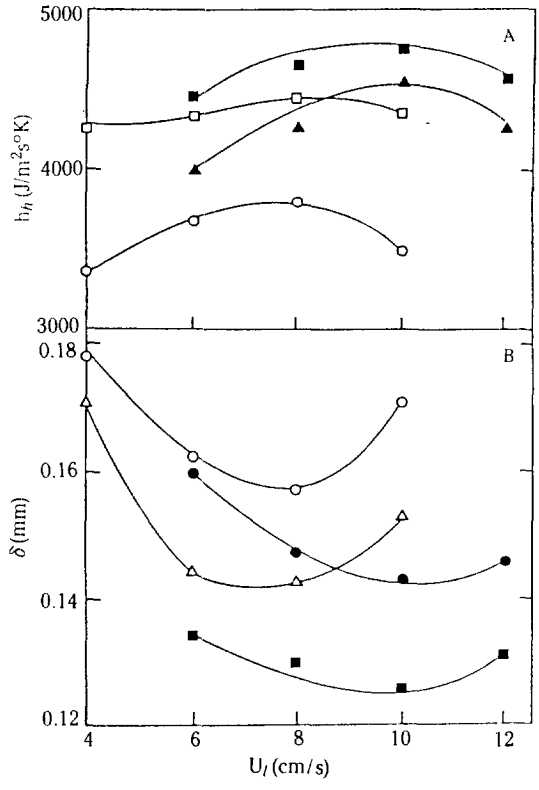

Fig. 4. Effect of liquid velocity on the average thermal boundary layer thickness and the heat transfer coefficient in the heater zone.

	○	△	□	●	▲	■	——
d_p(mm):	1.7	1.7	1.7	4.0	4.0	4.0	model
U_g(cm/s):	0.0	4.0	8.0	0.0	4.0	8.0	

since the larger particle has the higher minimum fluidizing velocity [20,21]. At the given gas velocity, an increase of liquid velocity may promote the mobility of particles in the heater zone which may results in higher contacting frequency between particles and the heater surface. Moreover, the fluid element velocity may also increase with liquid velocity. However, at higher liquid velocity, in contacting frequency of solic' with the heater surface may be reduced due to the considerable decrease in the solid concentration or phase holdup in the bed[13]. The reduction of solid phase holdup also causes the decrease in the turbulence which is generated by the fluidizing solid particles [22]. Therefore, the average boundary layer thickness around the heater increased at the higher liquid velocity. The similar trend has been observed by Richardson and Mitson[23] and Wasmund and Smith [4] in liquid fluidized beds. Since the heat transfer co fficients in the heater zone is inversely proportional to he boundary layer thickness(Eq. 15), the coefficient exhibits a maximum value with liquid velocity as shown in Fig. 4A.

The average boundary layer thickness around the heater goes through a minimum value with the variation of bed porosity in two and three phase fluidized beds (Fig. 5) where solid lines represent the calculated values. The data of Wasmund and Smith[4] in liquid fluidized beds also exhibit the same trend as shown in the figure. Since the heat transfer coefficient in the heater zone, h_h, is a function of gas and liquid velocities, it can be represented in terms of a modified Stanton number in the heater zone, St_{hM}, as defined in Eq. (16). The modified Stanton number in the heater zone decreased linearly with increasing bed porosity in two and three phase fluidized beds of different particle sizes (Fig. 6).

The heat transfer resistance in the fluidized bulk region, R_b, can be determined from Eq. (14) with the knowledge of the boundary layer thickness around the heater and the radial dispersion coefficient of liquid

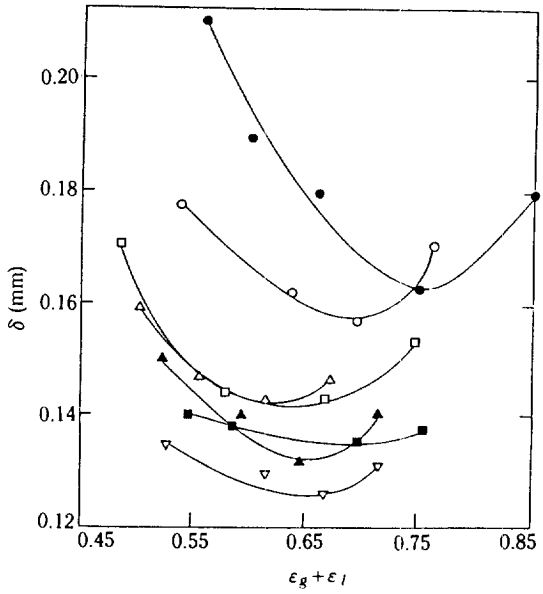

Fig. 5. Effect of bed porosity on the average thermal boundary layer thickness in liquid and three-phase fluidized beds.

	○	□	■	△	▲	▽	●	——
d_p(mm):	1.7	1.7	1.7	4.0	4.0	4.0	1.09	model
U_g(cm/s):	0.0	4.0	8.0	0.0	4.0	8.0	0.0	
	present study						Wasmund & Smith [4]	

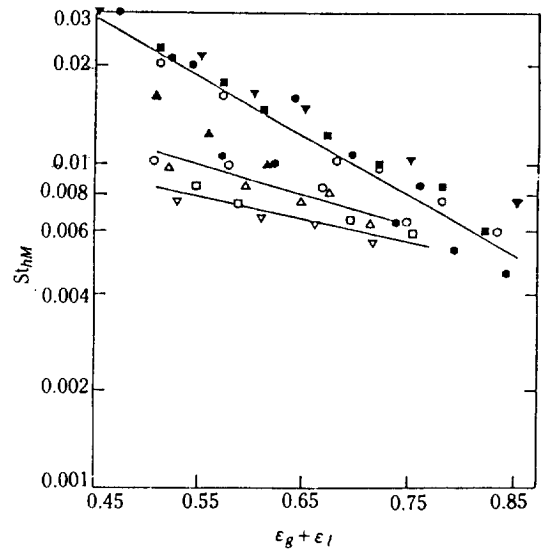

Fig. 6. Plot of modified Stanton number in the heater zone vs. bed porosity in liquid and three-phase fluidized beds.

	●	○	□	▲	△	▽	●	▼	■	○
d_p(mm):	1.7	1.7	1.7	4.0	4.0	4.0	1.3 lead	1.09	1.98	2.18
	glass beads						sphere	glass sphere		
U_g(cm/s):	0.0	4.0	8.0	0.0	4.0	8.0	0.0	0.0	0.0	0.0
	present study						Patel & Simpson [6]	Wasmund & Smith [4]		

phase, D_r, in the beds.

Recently, Kang and Kim[24] proposed a correlation for radial dispersion coefficient in three phase fluidized beds which is based on the isotropic turbulence theory;

$$Pe_r = \frac{d_p U_l}{D_r} = 28.3 \left(\frac{d_p}{D}\right)^{0.98} \left(\frac{U_l}{U_l+U_g}\right)^{1.16} \quad (20)$$

In the present analysis, the above correlation has been employed since the present experimental conditions are within the range of validity of the above Eq. (20). Thus obtained heat transfer resistance in the fluidized bed zone(Eq. 14) is shown with the experimental data (Table 1) in Fig. 7B.

The overall heat transfer resistance or the heat

Table 1. The average thermal boundary layer thickness around the heater, heat transfer resistances both in the heater and in the fluidized bulk zones and the overall heat transfer coefficient from the model equation

$d_p \times 10^3$ (m)	$U_g \times 10^2$ (m/s)	$U_l \times 10^2$ (m/s)	$D_r \times 10^{4*}$ (m^2/s)	$\delta \times 10^3$ (m)	$(1/h_h) \times 10^4$ (m^2sK/J)	$R_b \times 10^5$ (m^2sK/J)	$h_{cal.}$ (J/m^2sK)
1.7	0.0	4.0	1.8	0.179	3.00	1.97	3130
1.7	4.0	4.0	3.4	0.169	2.83	1.00	3413
1.7	4.0	8.0	5.1	0.142	2.38	0.70	4085
1.7	4.0	10.0	4.5	0.152	2.55	0.79	3810
1.7	8.0	10.0	6.0	0.136	2.28	0.59	4279
4.0	0.0	8.0	3.0	0.145	2.43	1.19	3926
4.0	4.0	8.0	4.8	0.138	2.31	0.74	4223
4.0	8.0	8.0	6.2	0.126	2.11	0.57	4615
4.0	8.0	10.0	6.9	0.125	2.09	0.52	4662
4.0	8.0	12.0	6.2	0.129	2.16	0.57	4511

* Kang and Kim [24]

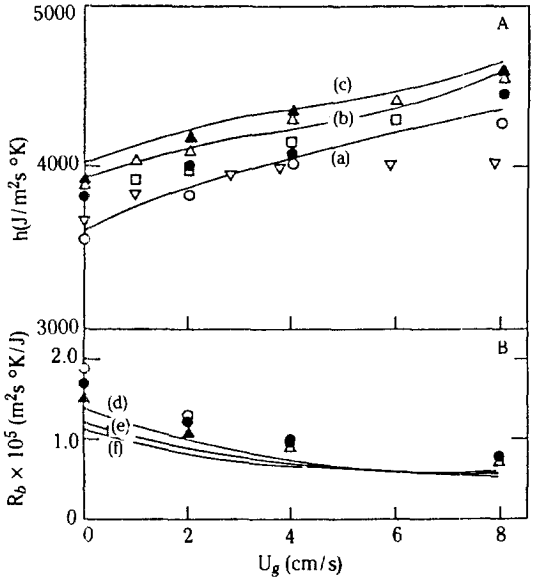

Fig. 7. Effect of gas velocity on the overall heat transfer coefficient and the fluidized bed resistance in liquid and three-phase fluidized beds.

	○	●	▲	a	b	c	d	e	f
d_p(mm):	1.7	4.0	4.0	1.7	4.0	4.0	1.7	4.0	4.0
U_g(cm/s):	8.0	8.0	10.0	8.0	8.0	10.0	8.0	8.0	10.0
	experiments			model					
d_p(mm):	3.0	4.0	4.0						
U_l(cm/s):	7.6	10.0	8.0						
	Chiu & Ziegler [10]			Kang et al. [13]					

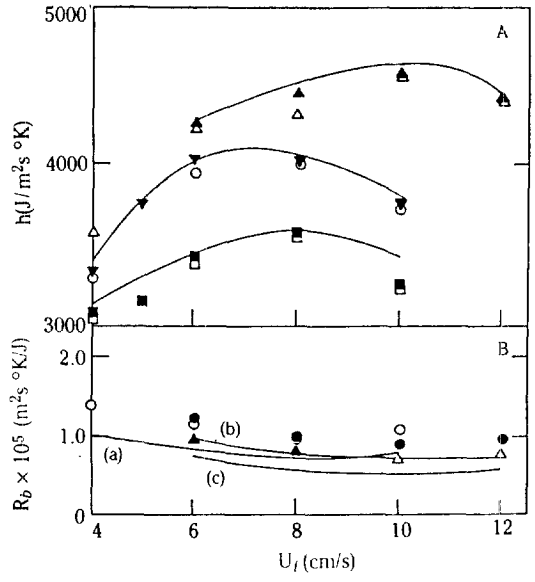

Fig. 8. Effect of liquid velocity on the overall heat transfer coefficient and the fluidized bed resistance in liquid and three-phase fluidized beds.

	○	△	□	●	▲	a	b	c	△	▼	■
d_p(mm):	1.7	1.7	1.7	4.0	4.0	1.7	4.0	4.0	4.0	1.7	1.7
U_g(cm/s):	4.0	8.0	0.0	4.0	8.0	4.0	4.0	8.0	8.0	4.0	0.0
	experiments					model			Kang et al. [13]		

transfer coefficient between an immersed heater and a three phase fluidized bed can be determined from Eq. (1) based on the two resistance model. The overall heat transfer coefficient in the bed increased with an increase in gas velocity and exhibits a maximum value with increasing liquid velocity as shown in Figs. 7A and 8A. However, the fluidized bed resistance decreased with increasing gas velocity (Fig. 7B) and exhibits a minimum value at a liquid velocity(Fig. 8B).

The overall heat transfer coefficient can be determined experimentally from Eqs. (17) and (18) with the knowledge of the radial temperature profile in the bed. These experimental values agree well with the values from the model Eq. (1) within the range of variation of gas and liquid velocities as shown in Figs. 7A and 8A. The resistance in the fluidized bulk zone can also be obtained from the experimentally determined overall heat transfer resistance and the heater zone resistance from Eq. (1). The fluidized bed resistance for heat transfer thus obtained decreased with increasing gas velocity(Fig. 7B) and exhibits a minimum value at a liquid velocity(Fig. 8B) or bed porosity(Fig. 9B) in two and three phase fluidized beds. In general, the experimentally determined bed resistances were larger than those of calculated values(Table 2). However, the resistance in the fluidized bulk zone, R_b, is relatively smaller than that in the heater zone, that is R_b values were in the range of 6-10 % and 3-5 % of the heater zone resistance in two and three phase fluidized beds, respectively, as can be seen in Figure 9 and Table 2. Therefore, the heat transfer in the heater zone is the rate controlling step for the overall heat transfer in two and three-phase fluidized beds(Fig. 2). It has been reported that the bed resistance account for about 10-50 % of the total heat transfer resistance in liquid fluidized beds[6].

This may imply that the bubble dispersion into the liquid fluidized bed can reduce the bed resistance appreciably so that the effective heat transfer can be obtained in three-phase fluidized beds.

The predicted overall heat transfer resistances or the overall heat transfer coefficients were in good agreement with the experimental values within the error range of 7%(Table 2). In Eq. (16), the constant K is approximately unity since it can be written as

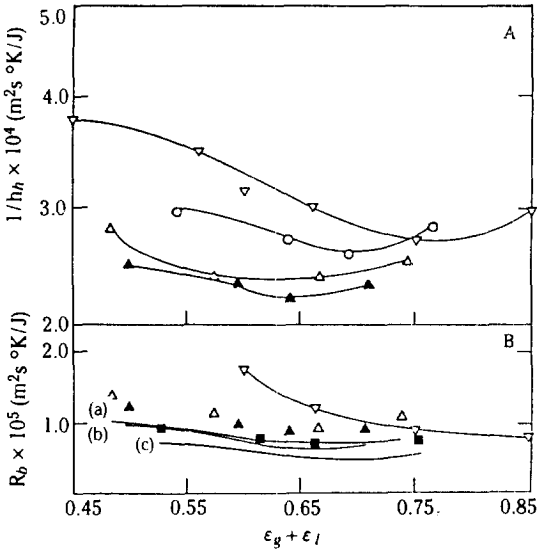

Fig. 9. Effect of bed porosity on the heat transfer resistances in the heater and fluidized bulk zones in liquid and three-phase fluidized beds.

	○	△	▲	■	a	b	c	▽
d_p(mm):	1.7	1.7	4.0	4.0	1.7	4.0	4.0	1.09
U_g(cm/s):	0.0	4.0	4.0	8.0	4.0	4.0	8.0	0.0
	experiments				model			Wasmund & Smith [4]

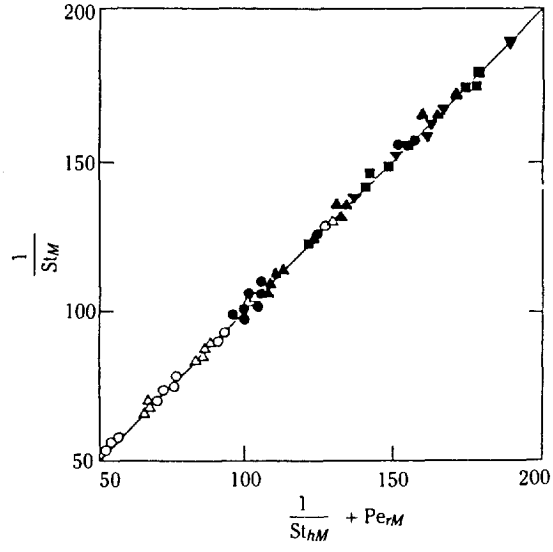

Fig. 10. Plot of $(1/St_M)$ vs. $\left(\frac{1}{St_{hM}} + Pe_{rM}\right)$ in liquid and three-phase fluidized beds.

	○	●	■	△	▲	▼
d_p(mm):	1.7	1.7	1.7	4.0	4.0	4.0
U_g(cm/s):	0.0	4.0	8.0	0.0	4.0	8.0

Table 2. Comparison of the average thermal boundary layer thickness around the heater, the ratio of the bed resistance to the heater zone resistance and the overall heat transfer coefficient between the calculated and measured values

$d_p \times 10^3$ (m)	$U_g \times 10^2$ (m/s)	$U_l \times 10^2$ (m/s)	$\delta_{cal}/\delta_{mea.}$	$\left(\frac{R_b}{1/h_h}\right)_{mea.}$	$\left(\frac{R_b}{1/h_h}\right)_{cal.}$	$h_{cal}/h_{mea.}$
1.7	0.0	6.0	1.012	0.088	0.065	1.010
1.7	0.0	8.0	1.006	0.073	0.052	1.014
1.7	0.0	10.0	1.006	0.080	0.056	1.068
1.7	4.0	6.0	0.993	0.048	0.034	1.020
1.7	8.0	6.0	0.993	0.034	0.024	1.017
1.7	4.0	8.0	0.993	0.040	0.029	1.018
1.7	8.0	8.0	0.985	0.034	0.025	1.025
1.7	4.0	10.0	0.992	0.043	0.031	1.018
1.7	8.0	10.0	0.993	0.036	0.026	1.017
4.0	0.0	8.0	0.986	0.068	0.049	1.033
4.0	0.0	10.0	0.994	0.063	0.046	1.024
4.0	0.0	12.0	0.985	0.065	0.050	1.029
4.0	4.0	6.0	0.987	0.050	0.039	1.025
4.0	8.0	6.0	1.004	0.042	0.031	1.003
4.0	4.0	8.0	0.986	0.043	0.032	1.033
4.0	4.0	10.0	1.008	0.040	0.029	1.003
4.0	8.0	10.0	0.992	0.034	0.025	1.017
4.0	4.0	12.0	0.979	0.040	0.031	1.032
4.0	8.0	12.0	0.985	0.036	0.026	1.025

$$K = \frac{1}{(R^2 - R_h^2)} \left\{ \frac{R^2 (R^2 \ln R - R_h^2 \ln R_h)}{R^2 - R_h^2} - R^2 \ln (R_h + \delta) + \frac{(R_h + \delta)^2}{2} - \frac{1}{4} (3R^2 + R_h^2) \right\} \quad (21)$$

Therefore, Eq. (16) can be reduced to

$$\frac{1}{St_M} = \frac{1}{St_{hM}} + Pe_{rM} \quad (22)$$

The agreement between the values from Eq. (22) and the experimental values are shown in Fig. 10 with the correlation coefficient of 0.985.

Since the modified Stanton and Peclet numbers were based on the fluid velocities($U_l + U_g$), Eq. (22) can be employed in liquid($U_g = 0$) and three-phase fluidized beds(Fig. 10).

CONCLUSIONS

(1) A two-resistance model can be used to analyze the heat transfer mechanism in two and three-phase fluidized beds. The heat transfer resistance in the heater zone is found to be predominant over that of the fluidized bulk zone in all the cases studied.

(2) The heat transfer resistances in the heater and the fluidized bulk zones decrease with an increase in gas velocity and particle size, whereas the resistances attained their minimum values as the liquid velocity and bed porosity in two and three-phase fluidized beds increase.

(3) The overall heat transfer resistance and the average thermal boundary layer thickness around the heater decrease with an increase in gas velocity and exhibited their minimum values as the liquid velocity and bed porosity in liquid and three-phase fluidized bed increase.

(4) The optimum bed porosity at which the maximum heat transfer coefficient is attained coincides with the bed porosity at which the boundary layer thickness around the heater attains its minimum value in two and three-phase fluidized beds.

ACKNOWLEDGEMENT

We acknowledge a grant-in-aid of research from the Korea Science and Engineering Foundation.

NOMENCLATURE

A : surface area of heater, m^2
C_{Pl} : heat capacity of liquid, J/kg K
D : column diameter, m
D_r : radial dispersion coefficient of liquid phase, m^2/s
D_z : axial dispersion coefficient of liquid phase, m^2/s
d_p : particle size, m
h : overall heat transfer coefficient, J/m^2 sK
h_h : heat transfer coefficient in the heater zone, J/m^2 sK
k_l : thermal conductivity of liquid phase, J/m sK
K : constant
L_h : heater length, m
$\dot{m}$: mass flow rate of liquid phase, kg/s
Pe_r : Peclet number in radial direction, $d_p U_l / D_r$
Pe_{rM} : a modified Peclet number in radial direction, $R_h(U_l + U_g)/D_r$
q : heat flow rate, J/s
q_h : heat flow rate from heater surface to bed per unit length of heater, J/s m
r : radial distance, m
R : radius of column, m
R_h : radius of heater, m
R_b : heat transfer resistance in fluidized bed zone, m^2sK/J
St_M : a modified Stanton number, $h/\{C_{pl}(U_l + U_g)\}$
T : temperature, K
T_b : boundary layer temperature, K
T_h : heater surface temperature, K
T_m : mean temperature of fluidized bed, K
U_g : superficial gas velocity, m/s
U_l : superficial liquid velocity, m/s
Z : axial direction

Greek Letters

ρ_l : liquid density, kg/cm^3
δ : average boundary layer thickness, m
μ : liquid viscosity, mPa.s
ε : phase holdup

Subscripts

b : boundary layer around heater
cal : calculated value
g : gas phase
h : heater
i : input
l : liquid phase
mea : measured value
M : modified
r : radial
s : solid phase
z : axial direction

REFERENCES

1. Deckwer, W.D.: *Chem. Eng. Sci.*, **35,** 1341 (1980).
2. Lewis, D.A., Fields, R.W., Xavier, A.M. and End-

wards, D.: *Trans IChem E.*, **60,** 40 (1982).
3. Chem, B.H. and McMillan, A.F.: *Can. J. Chem. Eng.*, **60,** 436 (1982).
4. Wasmund, B. and Smith, J.M.: *Can. J. Chem. Eng.*, **45,** 156 (1967).
5. Richardson, J.F., Ramani, M.N. and Shakiri, K.J.: *Chem. Eng. Sci.*, **31,** 619 (1976).
6. Patel, R.D. and Sinpson, J.M.: *Chem. Eng. Sci.*, **32,** 67 (1977).
7. Ostergaard, K.: "Fludization", 58. Soc. Chem. Ind., London (1964).
8. Viswanathan, S., Kaker, A.S. and Murti, P.S.: *Chem. Eng. Sci.*, **20,** 903 (1965).
9. Kato, Y., Kago, T., Uchida, K. and Morooka, S.: *Powder Technol.*, **28,** 173 (1981).
10. Chiu, T.M. and Ziegler, E.N.: *AIChE J.*, **29,** 677 (1983).
11. Muroyama, D., Fukuma, M. and Yasunishi, A.: *Can. J. Chem. Eng.*, **62,** 194 (1984).
12. Baker, C.G.J., Armstrong, E.R. and Bergougnou, M.A.: *Powder Technol.*, **21,** 195 (1978).
13. Kang, Y., Suh, I.S. and Kim, S.D.: *Chem. Eng. Commun.*, **34,** 1 (1985).
14. Kim, S.D., Kang, Y. and Kwon, H.K.: *AIChE J.*, **32,** 1397 (1986).
15. Suh, I.S., Jin, G.T. and Kim, S.D.: *Int. J. Multiphase Flow*, **11,** 255 (1985).
16. Kang, Y. and Kim, S.D.: *HWAHAK KONGHAK*, **25,** 81 (1987).
17. Kays, J.M.: "Convective Heat Transfer", McGraw-Hill, New York (1966).
18. Latif, B.A.J. and Richardson, J.F.: *Chem. Eng. Sci.*, **27,** 1933 (1972).
19. Edwards. D.K., Denny, V.E. and Mills, A.F.: "Transfer Processes", 2nd ed., Hemisphere Pub. Corp. (1979).
20. Kim, S.D., Baker, C.G.J. and Bergougnou, M.A.: *Can. J. Chem. Eng.*, **53,** 134 (1975).
21. Muroyama, K. and Fan, L.S.: *AIChE J.*, **31,** 1 (1985).
22. Schilichting, H.: "Boundary Layer Theory", McGraw-Hill, New York (1968).
23. Richardson, J.F. and Mitson, A.E.: *Trans. IChem E.*, **36,** 279 (1958).
24. Kang, Y. and Kim, S.D.: *Ind. Eng. Chem. Process Des. Dev.*, **25,** 717 (1986).